Title

Genetic architecture underlying variation in floral meristem termination in Aquilegia

Journal

Journal of Experimental Botany, 73(18)

ISSN

0022-0957

Authors

Min, Ya

Ballerini, Evangeline S

Edwards, Molly B

et al.

Publication Date

2022-10-18

DOI

10.1093/jxb/erac277

Peer reviewed

Journal of Experimental Botany, Vol. 73, No. 18 pp. 6241–6254, 2022
https://doi.org/10.1093/jxb/erac277 Advance Access Publication 22 June 2022

RESEARCH PAPER

Genetic architecture underlying variation in floral meristem termination in *Aquilegia*

Ya Min[1,†], Evangeline S. Ballerini[2], Molly B. Edwards[1], Scott A. Hodges[3] and Elena M. Kramer[1,*]

[1] Department of Organismic and Evolutionary Biology, Harvard University, Cambridge, MA, USA
[2] Department of Biological Sciences, California State University, Sacramento, Sacramento, CA, USA
[3] Department of Ecology & Marine Biology, University of California, Santa Barbara, CA, USA

[†] Present address: Department of Ecology and Evolutionary Biology, University of Connecticut, Storrs, CT, USA.
* Correspondence: ekramer@oeb.harvard.edu

Received 18 January 2022; Editorial decision 14 June 2022; Accepted 20 June 2022

Editor: Zoe Wilson, University of Nottingham, UK

Abstract

Floral organs are produced by floral meristems (FMs), which harbor stem cells in their centers. Since each flower only has a finite number of organs, the stem cell activity of an FM will always terminate at a specific time point, a process termed floral meristem termination (FMT). Variation in the timing of FMT can give rise to floral morphological diversity, but how this process is fine-tuned at a developmental and evolutionary level is poorly understood. Flowers from the genus *Aquilegia* share identical floral organ arrangement except for stamen whorl number (SWN), making *Aquilegia* a well-suited system for investigation of this process: differences in SWN between species represent differences in the timing of FMT. By crossing *A. canadensis* and *A. brevistyla*, quantitative trait locus (QTL) mapping has revealed a complex genetic architecture with seven QTL. We explored potential candidate genes under each QTL and characterized novel expression patterns of select loci of interest using *in situ* hybridization. To our knowledge, this is the first attempt to dissect the genetic basis of how natural variation in the timing of FMT is regulated, and our results provide insight into how floral morphological diversity can be generated at the meristematic level.

Keywords: *Aquilegia*, floral meristem termination, QTL, stamen whorl.

Introduction

Indeterminate growth is the foundation of development in all vascular plants and is achieved by the persistent activity of stem cells in meristems (Steeves and Sussex, 1989). Apical meristems in shoots and roots are highly organized structures that maintain a delicate, yet robust, balance between the production of stem cells and organogenic cells. In the flowering plants, when a plant enters the reproductive phase, the vegetative meristem transitions to inflorescence meristem (IM) identity, which then gives rise to floral meristem (FM) identity. Although their overall cellular organization is highly similar, this shift is accompanied by a number of transitions in the properties of the meristem, including changes in the rate and patterns of primordium production, and an eventual loss of indeterminacy.

The loss of indeterminacy in the FM is a well-regulated process, termed floral meristem termination (FMT), which is crucial and universal to the development of all flowers (Fig. 1). A

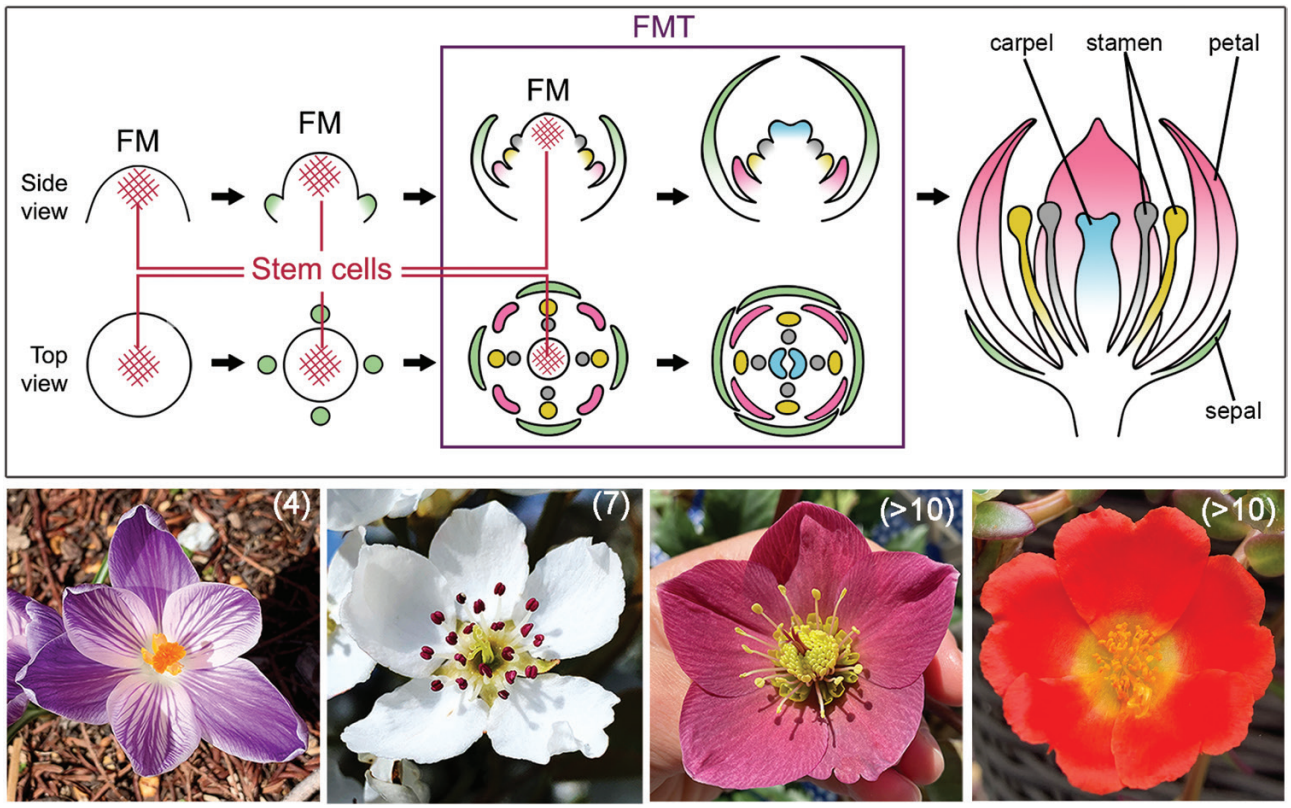

Fig. 1. FMT is an important and fine-tuned developmental process that occurs in all flowers. Upper panel: diagram of floral organ initiation and FMT during flower development. Organs of the same whorl share the same colors. Lower panel: example of four flowers with different whorl numbers. From left to right: *Crocus vernus* 'Pickwick', *Pyrus communis*, *Helleborus orientalis*, and *Portulaca umbraticola.* Numbers in parentheses indicate the number of whorls (or ranks for *H. orientalis*) of floral organs in each flower. Photos of *C. vernus*, *P. communis*, and *P. umbraticola* were taken by Ya Min, and the photo of *H. orientalis* was taken by Evangeline S. Ballerini.

typical flower has four types of floral organs: sepals, petals, stamens, and carpels, which are arranged from the outermost to the innermost positions of a flower (Fig. 1). Although the central stem cells stay active during the early phases of floral organ primordia initiation, this activity will cease at a specific time point, after which all remaining meristematic cells will be incorporated into the development of the innermost organs, the carpels (Steeves and Sussex, 1989). The precise control of FMT is critical to ensuring that the flower has the correct number of organs, and variation in FMT timing is an important source of floral morphological diversity and novelty. For some species, such as *Arabidopsis thaliana*, FMT occurs relatively quickly, and only four whorls of floral organs are produced. In many other taxa, FM activity is maintained for a more extended period; species from the Magnoliaceae, Monimiaceae, Nelumbonaceae, Nymphaeaceae, Papaveraceae, and Ranunculaceae, for instance, can have hundreds of spirally arranged or whorled floral organs (Endress, 1990; Fig. 1). Moreover, increased numbers of floral organs can create raw materials for the evolution of new organ types, such as the sterile staminodes observed in *Aquilegia* (Ranunculaceae) or *Mentzelia* (Loasaceae) (Walker-Larsen and Harder, 2000). The diversity in floral morphology of >300 000 angiosperm species is seemingly infinite, but one of the few major evolutionary trends that is independently observed in the transition from early-diverging angiosperms to either the core eudicot or monocot lineages is the transition from variable to stable whorl numbers in a flower (Endress, 1990), which is directly determined by the timing of FMT. Therefore, understanding how FMT is regulated in different angiosperm lineages is interesting from both developmental and evolutionary perspectives.

Currently, we have relatively good knowledge of the genes that are responsible for maintaining and terminating stem cell activities in *A. thaliana*. In the FM, the maintenance of the stem cell population is achieved by a feedback loop between the homeodomain protein WUSCHEL (WUS) and the CLAVATA (CLV) ligand–receptor system, in which WUS promotes central stem cell activity and induces the expression of the CLV3 peptide, while activation of the CLV signaling pathway represses the expression of *WUS* (Schoof *et al.*, 2000; Lenhard, 2003; Müller *et al.*, 2006). Meanwhile, in the early developing FM, the expression of the C class organ identity gene *AGAMOUS* (*AG*) is induced by WUS, while *AG* specifies the identity of stamens and carpels and is also responsible for the down-regulation of *WUS* expression (Lenhard *et al.*, 2001). Although the broad conservation of the *WUS–CLV*

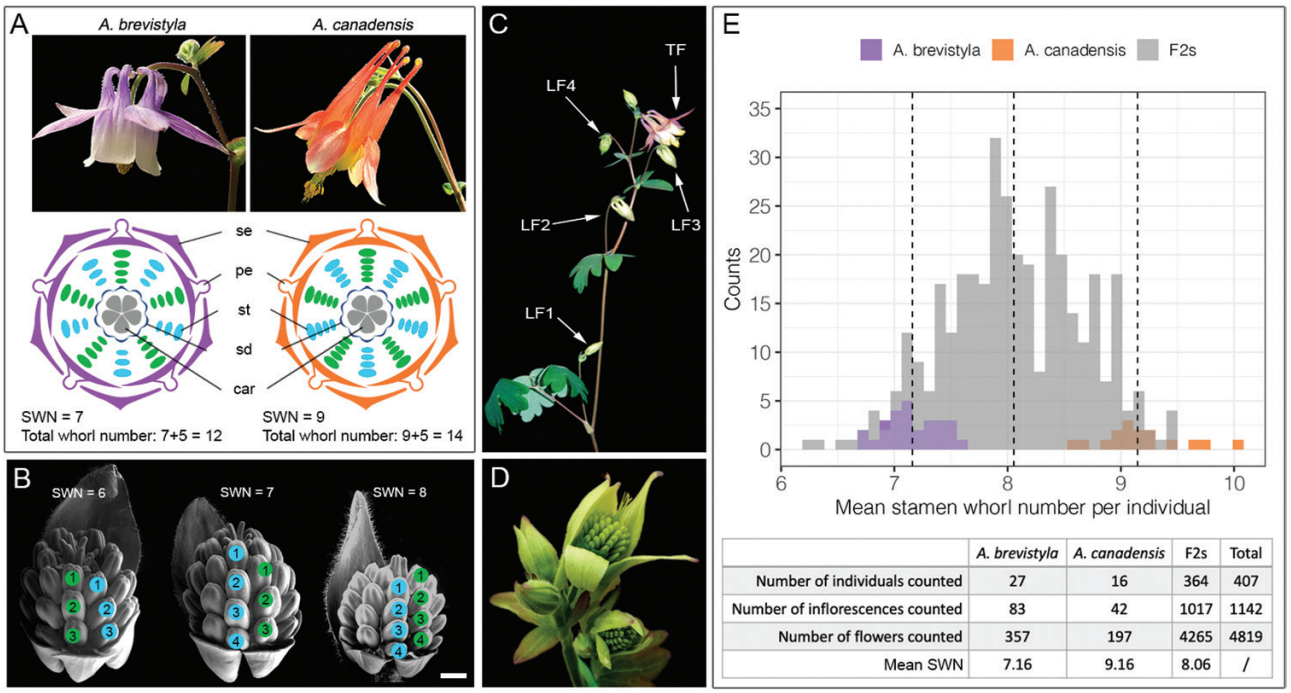

	A. brevistyla	*A. canadensis*	F2s	Total
Number of individuals counted	27	16	364	407
Number of inflorescences counted	83	42	1017	1142
Number of flowers counted	357	197	4265	4819
Mean SWN	7.16	9.16	8.06	/

Fig. 2. Phenotyping SWN in the parental and F2 populations. (A) Photos of flowers and floral diagrams of *A. brevistyla* and *A. canadensis*. (B) Examples of three F2 flower buds with different SWN. (C) Flowers that were sampled per inflorescence. (D) Developmental stages for which SWN was counted. (E) Histogram and summary statistics of SWN distribution in parental species and the F2s. In (A) and (B), stamen whorls positioned above the sepals are colored in blue while stamen whorls positioned above the petals are colored in green. Scale bar in (B)=100 μm. se, sepals; pe, petals: st, stamens; sd, staminodes; car, carpels.

and *WUS–AG* feedback loops has been demonstrated in diverse plant taxa (Nardmann and Werr, 2006; Litt and Kramer, 2010; Whitewoods *et al.*, 2020), the exact mechanisms by which AG controls the precise timing of *WUS* down-regulation have only been investigated in *A. thaliana* and tomato (*Solanum lycopersicum*). Specifically, AG activates the expression of a C2H2 zinc-finger transcription factor gene, *KNUCKLES* (*KNU*), whose protein product directly represses *WUS* (Payne, 2004; Sun *et al.*, 2009; Bollier *et al.*, 2018). Accurate timing of FMT is achieved because the activation of *KNU* by AG takes approximately two rounds of cell divisions, during which the stamen primordia are initiated. Once *WUS* down-regulation is achieved, all of the cells remaining in the center of the FM are incorporated into the carpel primordia (Sun *et al.*, 2009). Thus, FMT is tightly connected to the expression of *AG* and, moreover, the production of carpels in the center of the flower. It is perhaps not surprising that when we examine variation in FMT across the angiosperms, this is primarily expressed as variation in the number of stamen whorls produced before the final production of carpels and the concomitant termination of the meristem (Endress, 2011; Ronse De Craene, 2018).

However, integral to the known mechanism of *KNU* activation is that it only allows for one stamen and one carpel whorl to be produced in a flower. This begs the question of whether this pathway is conserved in systems that have more than four whorls of floral organs. Unfortunately, all currently established model systems (and their close relatives) belong to lineages that exhibit no variation in their floral whorl numbers, while most of the plant taxa exhibiting such variation do not have genomic or genetic resources or functional tools. To that end, species in the genus *Aquilegia*, a member of the buttercup family (Ranunculaceae), are well suited for investigating this fundamental developmental process. There are ~70 *Aquilegia* species, which share low interspecific sequence divergence and a high degree of interfertility due to having arisen via a recent adaptive radiation (Filiault *et al.*, 2018). Organs in *Aquilegia* flowers are produced in a whorl of five that are arranged in 10 orthostichies (vertical rows of organs), with alternate orthostichies positioned directly above either the sepals or the petals (Fig. 2A). Across species there is a consistent number of whorls for the sepals, petals, staminodes (with the exception of *A. jonesii*, which lacks staminodes; Munz, 1946), and carpels, but the number of stamen whorls varies both within and between species.

Aquilegia brevistyla and *A. canadensis* are North American sister species that vary in many pollination-related traits (Fig. 2A; Bastida *et al.*, 2010; Fior *et al.*, 2013; Edwards *et al.*, 2021), but also in what we term stamen whorl number (SWN). We argue here that this trait can be directly translated into variation in the timing of FMT: if the FM transitioned to carpel production and terminated earlier, there will be a smaller SWN compared with a flower in which the FM proliferates

for a longer period. Using SWN as a quantitative trait, we conducted quantitative trait locus (QTL) mapping in the resultant F2 generation from crossing *A. brevistyla* and *A. canadensis*. Our results reveal a complex genetic architecture with seven QTL, which we have associated with potential candidate genes under each QTL. To our knowledge, this is the first study to dissect the genetic basis of how natural variation in the timing of FMT is regulated, and our results highlight molecular pathways that may contribute to the regulation of FMT in *Aquilegia*.

Materials and methods

Plant material and growth conditions

Aquilegia brevistyla and *A. canadensis* seeds were collected from wild populations in Alberta (Canada) and Ithaca (NY, USA), respectively. One *A. canadensis* (pollen recipient) was crossed with one *A. brevistyla* (pollen donor) to generate the F1 generation. Five F1s were self-fertilized to generate the F2 population. All F2 seeds were stratified at 4 °C in the dark for 2–4 weeks, germinated in wet soil, and transplanted in individual pots. All plants were vernalized at 4 °C for 2 months to induce flowering. The parental and F1 individuals were grown in the greenhouse of the University of California Santa Barbara, and the F2 populations were grown in the greenhouses of Harvard University. All greenhouses used the same light and temperature conditions to achieve a 16 h/8 h (day/night) photoperiod at 18 °C and 13 °C.

Seeds of *Aquilegia*×*coerulea* 'Kiragami' were purchased from Swallowtail Garden Seeds (Santa Rosa, CA, USA), germinated in wet soil, and grown under the same 18 °C/13 °C (day/night) condition as described above. Once the plants developed approximately six true leaves, they were transferred into vernalization conditions (16 h daylight at 6 °C and 8 h dark at 6 °C) for 3–4 weeks, and then moved back to the regular growth conditions to promote flowering.

Meristem width measurement

The entire inflorescences of at least six individuals of each parental species were collected and fixed in FAA (10% formaldehyde, 50% ethanol, 5% acetic acid), and stored at 4 °C. Samples were then dehydrated through a graded ethanol series to 100%, transferred to 100% CitriSolv, and embedded in Paraplast Plus (Sigma-Aldrich). Embedded tissues were sectioned to 8 μm thick ribbons with a rotary microtome, stained in 0.1% Toluidine Blue O solution following the protocol described in Ruzin (1999), and mounted in Permount Mounting Medium (Fisher Scientific). Sections were then imaged using the Axio Zoom Microscope at the Harvard Center for Biological Imaging. The width of each floral meristem section was measured using ImageJ. Three to six serial sections were measured for each FM, and at least three FMs were measured for each developmental stage of each species. All FMs that were measured were non-terminal flowers, and the number of non-sepal primordia captured by the section was counted.

Phenotyping

For each plant, the SWN of the terminal flower and lateral flowers 1 to 4 from the first three inflorescences were counted (Fig. 2C). If flowers of these positions in an inflorescence were damaged/undeveloped, flowers at other positions were counted to achieve a total number of five flowers per inflorescence. If an inflorescence produced less than five flowers, all flowers were counted. SWN was counted when the flowers reached ~1–2 cm in length (Fig. 2D) because, at that developmental stage, all the stamens were arranged in vertical rows, which simplified counting.

Genotyping

Detailed genotyping information can be found in Edwards *et al.* (2021). Briefly, the DNA of the two parents that generated the cross was extracted from flash-frozen young leaves using the NEBNext Ultra II kit (NEB) and sequenced to ~40× coverage as 150 bp reads on an Illumina MiSeq at the Biological Nanostructures Lab in the California NanoSystem Institute at UC Santa Barbara. DNA of F2s was extracted from silica-dried young leaves using Qiagen DNEasy reagents and Magattract beads (Qiagen, Inc.); libraries were prepared following the protocol of the RipTide High Throughput Rapid DNA Library Preparation kit (iGenomX, CA, USA). The F2 libraries were pooled and sequenced at the Vincent J. Coates Genomics Sequencing Laboratory (UC Berkeley) using the NovaSeq 6000 platform to generate 150 bp paired-end reads. Samples were multiplexed to generate ~1–2× coverage. All sequence data are deposited in the Sequence Read Archive under BioProject ID PRJNA720109. Scripts and genotype/phenotype data are available at: https://github.com/anjiballerini/can.x.brev/.

Sequences were aligned to the *A. coerulea* 'Goldsmith' v3.1 reference genome (https://phytozome.jgi.doe.gov) using the Burrows–Wheeler aligner (Li and Durbin, 2009), and variable sites in the parents were identified using SAMtools 0.1.19 (H. Li *et al.*, 2009) with custom scripts used to identify the positions and genotypes at which the parents were homozygous for different alleles. These sites were used to assign reads in the F2s as having either *A. canadensis* or *A. brevistyla* ancestry. To determine the genotypes of the F2s, the genome sequences were binned into 0.5 Mb regions with moderate to high recombination frequencies and 1 Mb in regions with low or no recombination, and the frequency of reads with ancestry for each F_0 parent was used to determine the genotype of the bin. These bins and genotypes were used as markers to construct a genetic map and conduct QTL mapping. This genotyping method has been implemented in Filiault *et al*, (2018), Ballerini *et al.* (2020), and Edwards *et al.* (2021).

Mapping

After filtering out individuals and markers with >10% of information missing due to sequencing quality, we retained a total of 366 individuals and 620 markers. A genetic map of the seven chromosomes was then constructed following the protocol of the R/qtl package v1.46-2 (Broman *et al.*, 2003), with an error probability rate of 0.001 and 'kosambi' map function. Standard interval mapping with Haley–Knott regression (function 'scanone') was used for the initial mapping searching for potential QTL. The best multiple-QTL models are produced and selected by using function 'stepwiseqtl', which implements penalties on different interactions and drops one of the current main effects or interactions in each round of model comparison. Interactions among potential QTL and between QTL and covariance were detected with a two-dimensional genome scan (function 'scantwo'). Using the estimated positions of QTL from 'scanone', 'stepwiseqtl', and 'scantwo' as the input, the positions of QTL were refined by using the function 'makeqtl' and 'refineqtl', which then fit with a defined multiple-QTL model (function 'fitqtl') with all detected interactions. F1-parent-of-origin was used as covariance in all the tested mapping models. Position and effect size of QTL were estimated using drop-one-term ANOVA in the best-fitting model. The chromosome diagram with potential candidate genes (Fig. 4) was produced by using the LinkageMapView (Ouellette *et al.*, 2018).

In situ hybridization of genes of interest

Variable regions of the genes of interest were amplified by PCR (primers in Supplementary Table S1) from young inflorescence cDNA of *Aquilegia*×*coerulea* 'Kiragami'. The PCR products were cloned into the pCR™4-TOPO vectors, sequenced to confirm

identity, and reverse transcribed using T3 or T7 RNA polymerase and DIG RNA labeling mix (Sigma-Aldrich). Probe qualification and *in situ* hybridization steps followed Kramer, (2005). Slides were stained in calcofluor white for 5 min before imaging, and pictures were taken using the ZEISS Axio Zoom at the Harvard Center for Biological Imaging.

Statistical analysis

All statistical analyses (e.g. ANOVA andTukey's HSD) were performed using R (version 1.1.456).

Gene trees

Homologs of *AqROXYa* and *AqATH1* from various taxa were obtained by using BLAST on Phytozome (https://phytozome-next.jgi.doe.gov/). Multiple sequence alignments and Neighbor–Joining phylogenetic trees were constructed using Geneious Prime (v2021.1.1). We did not construct phylogenetic trees for other potential candidate genes because their homologs in *A. coerulea* and *A. thaliana* were each other's reciprocal top BLAST hits.

Results

SWN variation in the parental species and the F2s

We counted the SWN from 357, 197, and 4265 flowers from 27, 16, and 364 *A. brevistyla*, *A. canadensis*, and F2 individuals, respectively (Fig. 2). The SWN per individual of the parental species did not overlap: the mean SWN of *A. brevistyla* ranges from 6.69 to 7.57; that of *A. canadensis*, from 8.54 to 10; and that of the F2s, which overlapped with the range of both parental species, from 6.20 to 9.50 (Fig. 2E). The mean SWN for all *A. brevistyla*, *A. canadensis*, and F2s was 7.16, 9.16, and 8.06, respectively. Subsequently, we analyzed whether the position of flowers on the inflorescence is associated with their SWN. Flower position had a significant effect on the SWN for both parental species but not for the F2s (Supplementary Fig. S1). Given lower germination rates of interspecific hybrid seeds, seeds generated by selfing five different F1 plants (all of which had the same

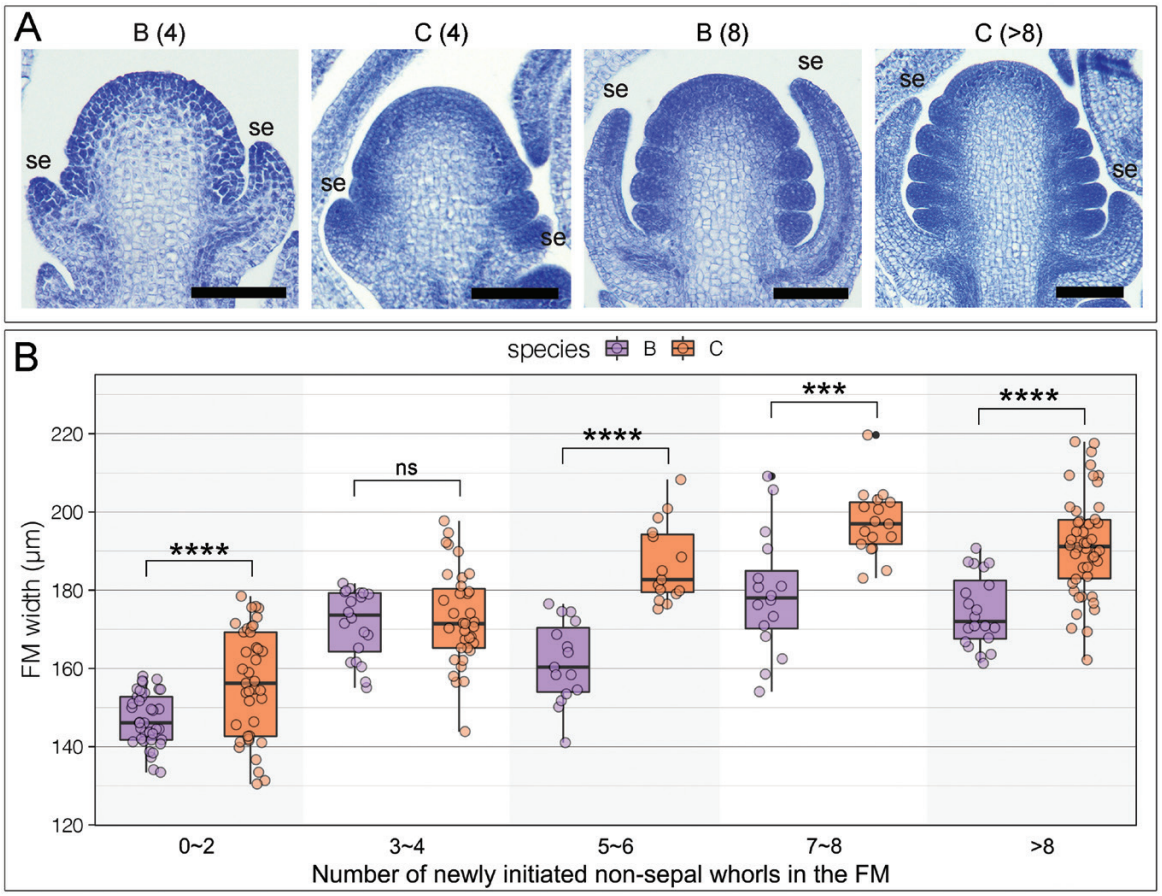

Fig. 3. FM width measurements of the parental species during the early developmental stages. (A) Examples of FM morphologies in *A. brevistyla* and *A. canadensis* at early developmental stages. Numbers in parentheses indicate the number of newly initiated stamen whorls in each FM. Scale bars=100 µm. (B) Comparison of FM width of different developmental stages between *A. brevistyla* and *A. canadensis*. Each data point represents a measurement of an FM width from a section. Three to six continuous sections were measured for each FM, and at least three FMs were measured for each developmental stage of each species. Comparison of FM widths of each stage between the parental species was done using Tukey's HSD. ns, not significant; ***P-value <0.001; ****P-value <0.0001; se, sepal; B, *A. brevistyla*; C, *A. canadensis*.

parents) were used to obtain 364 F2 progeny that reached the flowering stage (n=53–81 per F1). One-way ANOVA revealed that the SWN of the F2s differed significantly between the F1 parents (Supplementary Fig. S2). Lastly, we also analyzed the variation of SWN among flowers of the same plants. Interestingly, a small portion of *A. brevistyla* (7.4%), *A. canadensis* (18.8%), and F2s (6%) showed no variance in the SWN across all flowers counted within an individual, and this phenomenon was dependent on neither the number of flowers counted per individual plant (Supplementary Fig. S3; Pearson's correlation=0.052, t=0.98418, df=345, P=0.3257) nor the F1-parent-of-origin of the F2s (Supplementary Fig. S3). No significant correlation between the mean SWN per individual and the SD of SWN per individual was detected (Pearson's correlation=0.035, t=0.70438, df=404, P=0.4816).

Floral meristem size

To determine whether the initial FM sizes were different between the parental species, we measured the widths of FMs of the parental species at their earliest developmental stages (Fig. 3A). In general, the FMs of *A. canadensis* appeared to be slightly, but significantly, wider than those of *A. brevistyla* throughout the early developmental stages (Fig. 3B; Supplementary Table S2). The average FM widths of *A. brevistyla* and *A. canadensis* before the initiation of carpel primordia were 174.68 μm and 191.67 μm, respectively (Supplementary Table S2). Interestingly, the temporal developmental windows for significant FM size expansion seemed to be longer in *A. canadensis* than in *A. brevistyla* (Fig. 3B; Supplementary Table S2). The significant increase in widths of *A. brevistyla* FMs occurred when there were 0–4 whorls of non-sepal floral organs initiating, while the significant increase in the widths of *A. canadensis* FMs encompassed a larger developmental period, ranging from the stages that there were 0–6 whorls of non-sepal floral organs initiating (Supplementary Table S2).

Genetic architecture underlying stamen whorl variation

The genetic map was constructed using a total of 620 genetic markers, which fell into seven linkage groups, matching the n=7 chromosomes in the *Aquilegia* genome (Supplementary Fig. S4). We recovered seven major QTL using the mean

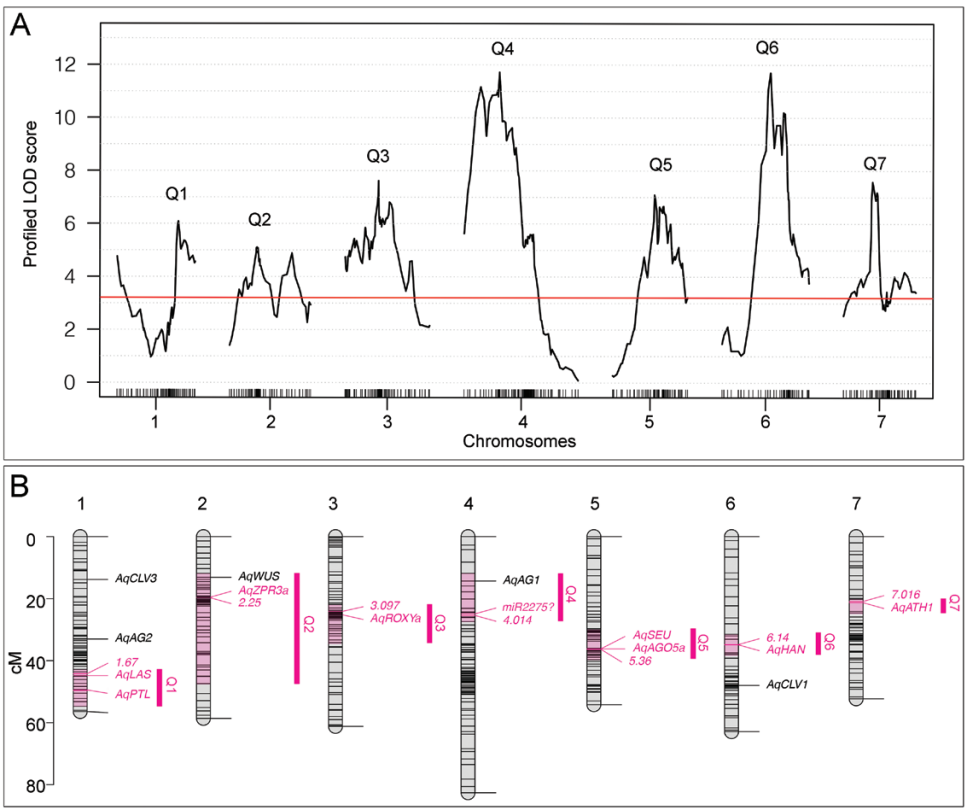

Fig 4. Genetic architecture and candidate genes. (A) LOD scores across seven chromosomes. Red line: α=0.05 genome-wide significance cut-off based on 1000 permutations. (B) Locations of QTL interval (pink regions on the chromosomes and magenta vertical bars), candidate genes, and genetic markers. All the genetic markers were named in numeric forms (e.g. 1.67 and 2.25) and only markers with the highest LOD scores under each QTL are shown.

SWN per individual as a phenotype and the F1-parent-of-origin as a covariate, with one QTL on each chromosome (Fig. 4A; Table 1). The difference in LOD scores between models that included or excluded the covariate are diminutive on all chromosomes (ranging from –0.3 to 0.49; Supplementary Fig. S5A), indicating no significant interaction between the QTL and the covariate. While several LOD profiles from a single QTL model suggested that there may be two QTL on a chromosome, a two-dimensional genome scan failed to detect evidence for the presence of more than one QTL on a single chromosome (Supplementary Table S3). The presence of only one true QTL on chromosome 2 was further confirmed by controlling the two potential QTL: when the true QTL (i.e. Q2) was controlled, the presence of the second peak also disappeared (Supplementary Fig. S5B). We did detect significant interactions between two pairs of QTL: Q3 and Q7, and Q1 and Q6 (Supplementary Fig. S5C), and thus incorporated these interactions in the full QTL model (Table 1).

The full QTL model had a total LOD score of 48 and explained 46.5% of the observed phenotypic variation (Table 1). Q3, Q4, and Q5 exhibit larger additive effects than dominant effects, while the remaining QTL have larger dominant effects on the phenotypic variation (Fig. 4A; Table 1; Supplementary Fig. S6). The phenotypic variation explained by each QTL and the QTL interactions was very similar, with Q4 and Q6 having the largest additive and dominant effects, respectively, and each explained 8.8% of the phenotypic variation (Table 1). This suggested that the genetic architecture of SWN is a complex trait controlled by multiple loci, each with small effect.

Potential candidate genes

In order to identify potential candidate genes underlying these QTL, we examined the genomic regions defined by markers that flanked the 95% Bayesian credible interval of each QTL, which was calculated by using the posterior distribution of 10^{LOD} on a given chromosome. The genomic regions of Q1, Q4, Q6, and Q7 were <6 Mb in size, while those of Q2, Q3, and Q5 were >20 Mb (Supplementary Table S4). Among all the QTL, Q6 and Q2 had the smallest (1.5 Mb) and the largest (36.5 Mb) intervals, containing 226 and 3242 genes, respectively (Supplementary Table S4). We sought to identify loci for further study under each QTL based on (i) the locations of the annotated genes relative to the location of the markers with the highest LOD scores, (ii) homology to previously studied loci related to meristem function, and (iii) gene expression levels during early FM developmental stages using previously published RNA-sequencing (RNAseq) data for *A. coerulea* 'Kiragami', which sampled developmental stages covering the FMT window (Min and Kramer, 2020). Because our genotyping method used 0.5 Mb or 1 Mb binned genomic regions as the genetic markers rather than single nucleotide markers (see details in the Materials and methods), we gave the highest priority to genes located in the region of the marker with the highest LOD scores.

Table 1. Summary statistics for QTL

		Full model result:								
		y~Q1+Q2+Q3+Q4+Q5+Q6+Q7+Q1:Q6+Q3:Q7								
			df	**Type III SS**	**MS**	**LOD**	**PVE**	***P*-value (*F*)**		
		Model	22	61.87	2.81	48.04	44.47	0		
		Error	331	71.27	0.22					
		Total	353	133.14						
Drop one QTL at a time ANOVA table										
	Chr	Position (cM)	df	Type III SS	LOD	PVE	*F*-value	*P*-value (*F*)	Add.	Dom.
Q1	1	44.233	6	5.87	6.1	4.4	4.6	<0.001	0.05	–0.16
Q2	2	19.676	2	4.89	5.1	3.7	11.4	<0.001	–0.07	0.2
Q3	3	24.050	6	7.43	7.6	5.6	5.7	<0.001	–0.11	–0.01
Q4	4	25.406	2	11.73	11.7	8.8	27.3	<0.001	–0.27	0.07
Q5	5	30.155	2	6.89	7.1	5.2	16.0	<0.001	–0.25	0.17
Q6	6	34.828	6	11.72	11.7	8.8	9.1	<0.001	–0.14	–0.27
Q7	7	20.944	6	7.38	7.6	5.6	5.7	<0.001	0	0.15
Q1×Q6			4	5.45	5.7	4.1	6.3	<0.001		
Q3×Q7			4	5.39	5.6	4.1	6.3	<0.001		
Estimated effects for QTL interactions										
Q1 (a)×Q6 (a): 0.01		Q1 (d)×Q6 (a): –0.23			Q1 (a)×Q6 (d): –0.38				Q1 (d)×Q6 (d): 0.45	
Q3 (a)×Q7 (a): 0.19		Q3 (d)×Q7 (a): 0.09			Q3 (a)×Q7 (d): –0.16				Q3 (d)×Q7 (d): –0.24	

Chr, chromosome; PVE, percentage variance explained; Add./(a), additive affects; Dom./(d). dominant effects.

Under Q1, we identified a homolog of *LATERAL SUPPRESSOR* (*LAS*), *AqLAS*, which is interesting because mutations in the *LAS* orthologs in *A. thaliana* and tomato severely impact axillary meristem activity, suggesting that the genes may influence indeterminacy (Schumacher *et al.*, 1999; Greb, 2003; Wang *et al.*, 2014). One additional gene that was located 3 Mb away from *AqLAS* also caught our attention: *AqPETAL LOSS* (*AqPTL*). *PTL* is a floral organ boundary gene in *A. thaliana* that controls cell proliferation (Griffith *et al.*, 1999; Brewer *et al.*, 2004; Lampugnani *et al.*, 2012). We considered *AqPTL* interesting for two reasons. First, PTL has been shown to physically interact with and be transcriptionally regulated by the C2H2 transcription factor gene *JAGGED* (*JAG*) (Sauret-Güeto *et al.*, 2013), whose *Aquilegia* homolog *AqJAG* has been shown to be critical to maintaining the FM (Min and Kramer, 2017). Second, PTL and the gene product of *HANABA TANARU* (*HAN*) interact by sharing JAG as a direct protein partner to regulate floral morphogenesis in *A. thaliana* (Ding *et al.*, 2015), and the homolog of *HAN* is a potential candidate gene under Q6 (Fig. 4B).

Interestingly, *AqWUS* is within the 95% Bayesian credible intervals of Q2, located at the edge of the interval (Fig. 4B). Since the expression of *AqWUS* has not been examined *in situ*, we analyzed its expression pattern during the early developmental stages of *A. coerulea* FM (Fig. 5A–E). *AqWUS* is expressed in a small population of cells in the center of the FM from the earliest stages (Fig. 5A–E). The expression in these central zone cells persists during the initiation of floral organs and disappears when carpel primordia start to initiate. These observations are consistent with the expression of *WUS* orthologs in all taxa examined to date (Nardmann and Werr, 2006; Galli and Gallavotti, 2016), suggesting functional conservation of *AqWUS* as well. However, the marginal position of *AqWUS* in Q2 makes it a less compelling candidate.

Within the highest LOD interval of Q2, which is located 8.7 Mb away from *AqWUS*, we identified another locus of interest, *AqLITTLE ZIPPER 3a* (*AqZPR3a*; Fig. 4B). *AqZPR3a* encodes a small leucine zipper-containing protein and is the homolog of the previously identified gene *ZPR3* in *A. thaliana* (Weits *et al.*, 2019). Homologs of the *ZPR* genes have been shown to regulate leaf polarity and shoot apical meristem maintenance in *A. thaliana* and tomato (Wenkel *et al.*, 2007; Kim *et al.*, 2008; Xu *et al.*, 2019), but little is known about whether they are involved in any FM-specific functions in these plant systems. In the *Aquilegia* FM, *AqZPR3a* exhibits dynamic expression patterns (Fig. 5F–L). At the earliest stages of the FM, concentrated expression of *AqZPR3a* is detected across the central epidermal layer, and moderate expression is found in the central zone (Fig. 5F). This strong expression in the epidermal layer persists until the FM has initiated several whorls of floral organs, but the width of the domain seems to contract as FM development proceeds (Fig. 5F–I). In contrast, the expression in the central zone disappears rapidly after initiation of the sepal primordia (Fig. 5F, G, H′, J′′). Strong expression of *AqZPR3a* is also detected at the adaxial boundary of all initiating floral organ primordia (Fig. 5H–J′′). However, these adaxial expression domains are restricted to the medial region of each primordium, rather than the entire abaxial surface, which can be seen in serial sections through the same FM (Fig. 5H, H′, J, J′, J′′). Strong but patchy expression of *AqZPR3a* is also detected in the adaxial epidermal layer of older lateral organs, such as the sepals (Fig. 5I, J, J′), petals (Fig. 5K), stamens (Fig. 5K), and carpels (Fig. 5K). Intriguingly, expression of the *ZRP* genes across the epidermal layers has never been observed in any other plant systems.

Under Q3, we identified *AqROXYa* which codes for a thioredoxin superfamily protein and is a homolog of *A. thaliana* genes *ROXY1* and *ROXY2* (Fig. 4B; Supplementary Fig. S7). In *A. thaliana*, *ROXY1* appears to be a negative regulator of *AG*, and the homolog of *ROXY* in maize appears to regulate shoot meristem size and phyllotaxy (Xing *et al.*, 2005; Yang *et al.*, 2015). In *Aquilegia*, expression of *AqROXYa* is detected across the FM at the earliest developmental stages (Fig. 5M), but this broad expression disappears once the primordia begin initiating. *AqROXYa* is detected in a restricted abaxial region of each emerging floral organ primordium but quickly declines once they begin to differentiate (Fig. 5M–O′). For instance, in an FM with several whorls of initiated stamen primordia, the expression of *AqROXYa* is only detected in the abaxial side of the innermost two whorls of emerging organ primordia (Fig. 5O, O′).

The confidence interval of Q4 spanned 3.8 Mb but only contained 176 annotated genes that were expressed in the RNAseq dataset (Supplementary Table S5). Tandem duplicates of the C-class gene homolog *AqAG1* are located at the edge of the genomic interval, quite distant from the marker with the highest LOD score (Fig. 4B). Within the 1 Mb region (4 800 000–5 800 000) that contained the genetic marker with the highest LOD, there were only 40 expressed genes, eight of which are *Aquilegia* specific without any annotated *A. thaliana* homologs, with most of the remaining genes annotated to be involved in plant defense and basic metabolic functions (Supplementary Table S6). Since a previous study showed that miRNA2275 (miR2275) precursors and 24-*PHAS* loci are significantly enriched in chromosome 4 compared with other chromosomes in *Aquilegia* (Pokhrel *et al.*, 2021b), we also searched for potential miRNA-encoding loci under Q4. MiR2275 is the primary miRNA that triggers phased, secondary, small interfering RNAs (phasiRNAs) of 24 nucleotides in length, and the production of 24-nt phasiRNAs requires both miR2275 copies and 24-*PHAS* loci as their targets (Liu *et al.*, 2020). We found that the region with the highest LOD under Q4 overlaps with the genomic region with the highest density of miR2275 precursors and *24-PHAS* loci, including three of the 11 annotated clusters of miR2275 precursors and 91 24-*PHAS* loci in total, comprising 31.7% of all 24-*PHAS* loci on chromosome 4 (~45.8 Mb) and 14.1% of such loci in the entire genome (~300 Mb) (Pokhrel *et al.*, 2021b).

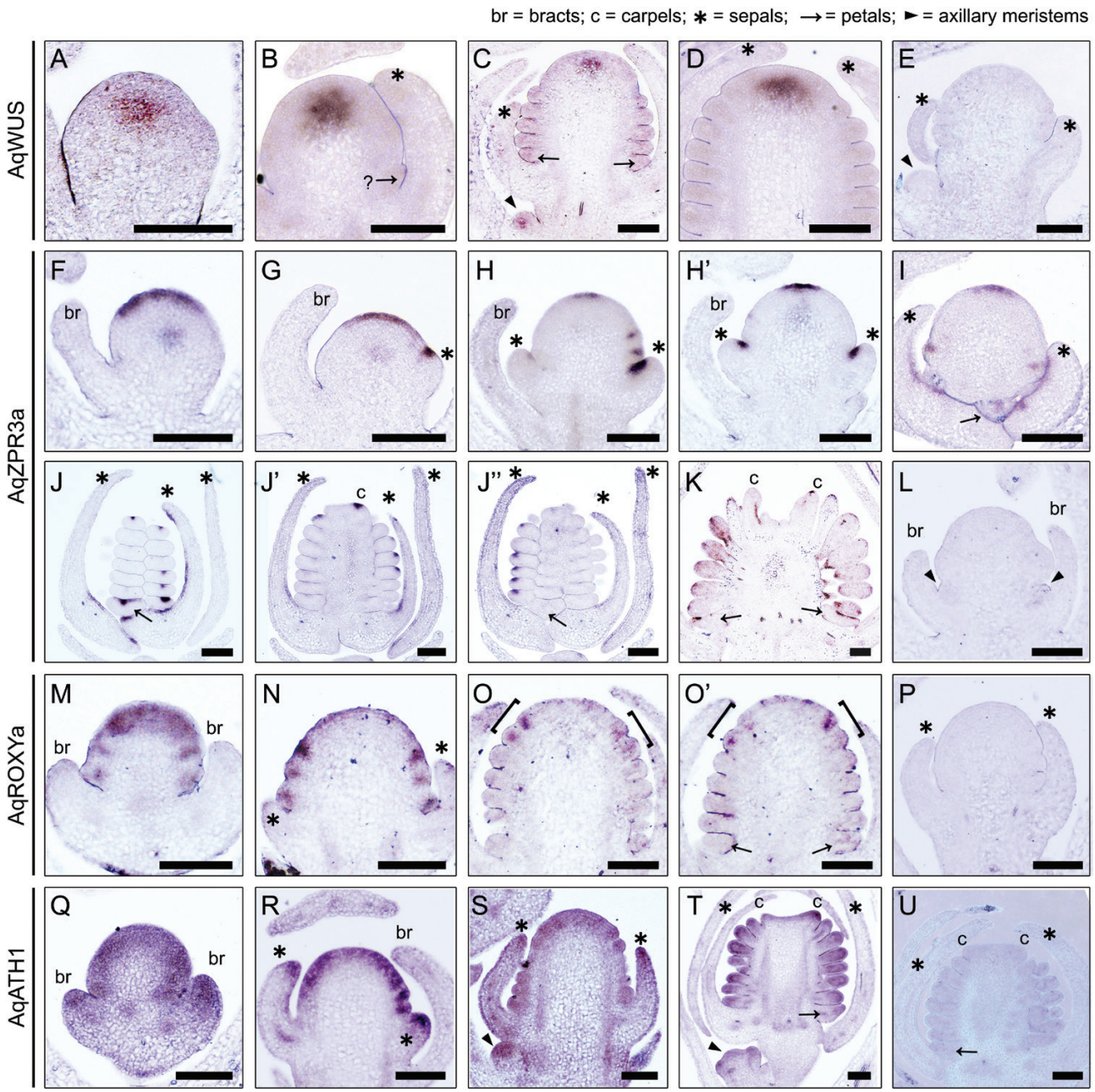

Fig 5. *In situ* hybridization of *AqWUS* and candidate genes. (A–E) Expression patterns of *AqWUS* (A–C) and its sense probe (E). (A) An FM that has not produced any organs. (B) An FM that is in the process of initiating either a petal primordium or the outermost stamen primordium (and thus indicated by an arrow with a question mark). (C) An FM that has at least eight whorls of stamens initiated; *AqWUS* expression was also detected in an axillary meristem (arrowhead). (D) An FM that has at least 11 whorls of stamens produced. (E) Sense probe of *AqWUS*. (F–L) Expression patterns of *AqZPR3a* (F–K) and its negative control probe (L). (F) An FM that has not produced any organs subtended by a bract (br). (G) An FM that has just started to produce sepal primordia (asterisk). (H, H′) Serial sections through the same FM that has only produced sepal primordia (asterisks). (I) An FM that has produced 1–2 whorls of stamens. (J, J′, J′′) Serial sections through the same floral bud that has initiated all floral organs. (K) A young floral bud in which all floral organs are differentiating. (L) Sense probe of *AqZPR3a*. (M–P) Expression of *AqROXYa* (M–O′) and its negative control (P). (M) An FM that has not produced any organs. (N) An FM that is in the process of initiating petal or utermost stamen primordia. (O, O′) Serial sections through the same FM, with brackets indicating newly emerging primordia. (P) Sense probe of *AqROXYa*. (Q–U) Expression of *AqATH1* (Q–T) and its negative control (U). (Q) An FM that has not produced any organs. (R) A young FM that is in the process of initiating petal and stamen primordia. (S) An FM initiating stamen primordia and an associated axillary meristem (arrowhead). (T) A floral bud with carpel primordia just initiated and an axillary meristem (arrowhead). (U) Sense probe of *AqATH1.* All scale bars=100 μm.

For Q5, there are two genes located within the highest LOD interval that have homologs that are known to function as FM regulators: *AqSEUSS* (*AqSEU*) and *AqARGONAUTE5a* (*AqAGO5a*). In *A. thaliana*, *SEU* is known to repress *AG* to regulate FM and organ patterning (Pfluger and Zambryski, 2004; Grigorova *et al.*, 2011; Wynn *et al.*, 2014), while in *Aquilegia*, *AqAGO5a* has been identified as a core hub gene associated with early FM development (Min and Kramer, 2020).

Under Q6, we located the homolog of *HANABA TANARU* (*AqHAN*). *HAN* codes for a GATA-type zinc finger transcription factor and, in *A. thaliana*, *HAN* is expressed at the organ boundaries, is known to regulate *WUS* expression, and directly interacts with a number of key genes in FM regulation and primordia initiation (Zhao *et al.*, 2004; Ding *et al.*, 2015). As mentioned above, we have detected significant interaction between Q1 and Q6 (Supplementary Fig. S5). We found it intriguing that HAN and PTL interact through JAG to control FM morphogenesis in *A. thaliana* (Ding *et al.*, 2015), since their *Aquilegia* homologs are located within the confidence interval of Q1 and Q6, respectively.

Lastly, *AqHOMEOBOX GENE 1* (*AqATH1*) is the only gene located within the highest LOD interval of Q7 that is annotated with a meristem-related function (Supplementary Fig. S8). In *A. thaliana*, *ATH1* regulates the boundary between the stem and the lateral organs, but is also involved in stem cell regulation in meristems by maintaining the expression of the meristem marker gene *SHOOT MERISTEMLESS* via a self-activation loop (Gómez-Mena and Sablowski, 2008; Li *et al.*, 2012; Cao *et al.*, 2020). *AqATH1* is broadly expressed across the *Aquilegia* FM throughout the early developmental stages (Fig. 5Q–T), in all early floral organ primordia (Fig. 5R), and at the distal tip of the young lateral organs such as the bracts (Fig. 5Q), sepals (Fig. 5R, S), and petals (Fig. 5T).

Discussion

Aquilegia *is an ideal system for studying FM regulation and termination*

Over recent decades, we have gained significant insight into various aspects of plant meristem development and function, but the regulation of FMT remains a poorly studied subject. This is despite the fact that FMT is an indispensable process in floral development, and variation in FMT timing is a key component of the generation of floral morphological diversity (Fig. 1). Progress in understanding the regulation and evolution of FMT is hampered due to the lack of natural variation in floral organ whorl numbers in all of our currently established model systems (and their close relatives), while taxa with such a variation generally lack the genomic and molecular resources to investigate this question further. To this end, *Aquilegia* can be an ideal system for studying FMT because species of *Aquilegia* share relatively low interspecific sequence variation combined with a high degree of interfertility thanks to its recent adaptive radiation (Hodges and Arnold, 1994; Filiault *et al.*, 2018). At the same time, they all share a consistent floral bauplan that only varies in SWN (Munz, 1946), and possess a fully sequenced and well-annotated genome along with RNAi-based methods for functional studies (Kramer, 2009; Filiault *et al.*, 2018). Recognizing that floral SWN is the best available quantitative trait to represent the timing of FMT, we utilized a genetic cross between two sister species differing in SWN, and sought to take the first step to explore the molecular basis of naturally occurring variation in the FMT timing. The mean SWN of *A. brevistyla* and *A. canadensis* is 7.16 and 9.16, respectively, and they do not overlap, while the mean SWN of their F2 progeny was found to encompass the entire range of the parental species (Fig. 2E).

One question we sought to explore was whether there is any difference in early FM growth dynamics between the parental species by analyzing developmental histological series of FMs (Fig. 3). Overall, we observe that the *A. canadensis* FMs (i) are larger in general, (ii) have a longer developmental window to increase FM width, and, yet, (iii) still make five stamens per whorl. There are numerous previous studies showing that an increase in FM diameter is often associated with an increase in floral organ number per whorl, rather than an increase in the number of whorls (e.g. Carles *et al.*, 2004; Fan *et al.*, 2014; Chu *et al.*, 2019). Of course, these studies typically rely on mutagenesis or gene overexpression rather than natural variation. This suggests that natural variation in meristem size relies on a greater degree of coordination such that meristem size changes in conjunction with the size of primordia inhibition fields, allowing the number of organs per whorl to stay constant. The current data do not allow us to distinguish between whether the *A. canadensis* FM is growing for a longer period (e.g. perhaps plastochrons are slower, allowing more mass to be accumulated between subsequent whorls) or proliferating at a faster rate. Given what we know about the role of cell division timing in influencing FMT, answering this question is important to understanding the FMT mechanism in *Aquilegia*. Future studies using a recently developed live imaging technique in *Aquilegia* (Min *et al.*, 2022) may allow us to compare growth rates between the initiation of successive whorls in these two species and better characterize this phenomenon.

Another curious observation regarding SWN is that we observed a small portion of individuals in both parental species as well as the F2s that exhibited no variation in SWN, regardless of how many flowers were counted on the plants. In contrast, most other individuals exhibited variation in SWN within an individual plant (Supplementary Fig. S3). This seems to suggest that there is variation in the robustness

of this trait between different individuals. Unfortunately, the fact that there was no significant divergence in this pattern between the parent species meant that we could not map it in the current study, but we hope that examination of within-inflorescence SWN canalization in other *Aquilegia* species will allow the identification of suitable models and the dissection of its genetic basis.

Variation in the timing of Aquilegia *FMT is controlled by multiple loci of small effects*

We recovered seven major QTL that are responsible for variation in SWN, with one QTL located on each chromosome, and the percentage of phenotypic variance explained by each QTL ranging from 3.7% to 8.8% (Fig. 4; Table 1). These results are comparable with those of previous studies in meristem-related traits of domesticated crops, particularly maize, which also revealed multiple QTL of small effects (Vlăduţu *et al.*, 1999; Upadyayula *et al.*, 2006; Bommert *et al.*, 2013; Thompson *et al.*, 2014, 2015). Interestingly, although all the meristem-related traits measured in maize were highly heritable, the total percentage of variance explained by all the QTL was never higher than 50% (e.g. Bommert *et al.*, 2013; Thompson *et al.*, 2014, 2015), suggesting that there are other loci with even smaller effects that were not picked up by the QTL mapping, which is a likely scenario for our current study as well.

We have identified potential candidate genes under the QTL (Fig. 4; Supplementary Table S6), and, further, uncovered novel FM expression patterns of *AqZPR3a* and *AqROXYa*, which were the loci of interest associated with Q2 and Q3, respectively (Figs 4, 5). In *A. thaliana* and tomato, expression of the *ZPR* genes is restricted to the adaxial region of lateral organs and the central zone of the shoot meristem, and the *ZPR* genes function in both establishing organ polarity and restricting the stem cell domain in the meristems by acting as post-translational suppressors of the class III HD-ZIP abaxial identity genes by inhibiting their homodimerization (Wenkel *et al.*, 2007; Kim *et al.*, 2008; Weits *et al.*, 2019; Xu *et al.*, 2019). However, we have also observed strong expression of *AqZPR3a* in the central epidermal layer of FMs throughout their early developmental stages (Fig. 5F–I), which has not been observed in any previous studies. It will be very interesting to determine whether this expression pattern indicates a novel function or is related to known ZPR functions in modulating meristem regulation. In the case of *ROXY* homologs in other models, expression has been found to be restricted to incipient and newly emerged organ primordia (Xing *et al.*, 2005; S. Li *et al.*, 2009; Yang *et al.*, 2015), but abaxialized expression such as what was found for *AqROXYa* has not been observed before. In *A. thaliana*, *ROXY1* is known to interact with *PTL* to regulate floral primordium initiation while, in maize, a *ROXY* homolog controls meristem size primordia (Xing *et al.*, 2005; S. Li *et al.*, 2009; Yang *et al.*, 2015); either of these functions could be important for controlling FMT in *Aquilegia*.

The Q4 locus is particularly intriguing because it explains the highest relative percentage of phenotypic variation, but it is also the QTL with the fewest obvious candidate genes to investigate (Supplementary Tables S4, S5). Chromosome 4 of *Aquilegia* appears to have followed a distinct evolutionary path from the rest of the genome and displays many unique features compared with the remaining six chromosomes, including having a higher proportion of genes arrayed in tandem and segmental duplicates, more genetic polymorphism and transposable elements, lower gene density, and reduced gene expression (Filiault *et al.*, 2018; Aköz and Nordborg, 2019). Although the *AqAG1* tandem duplication is included in the 95% Bayesian credible interval, it may be less likely to be the causative gene compared with other genes that were located closer to the highest LOD score marker. The lack of potential candidate genes under Q4 led us to consider other factors besides protein-coding genes, leading to the finding that the highest Q4 LOD interval overlaps with the region that harbors the most concentrated density of miR2275 precursors and 24-*PHAS* loci in the entire *Aquilegia* genome (Pokhrel *et al.*, 2021b). As the primary miRNA that triggers 24-nt phasiRNA, a pathway that is conserved across the angiosperms, miR2275 has been shown to be expressed in the reproductive tissues of various monocot and dicot lineages, particularly in developing anthers (Zhai *et al.*, 2015; Fei *et al.*, 2016; Kakrana *et al.*, 2018; Pokhrel *et al.*, 2021a, b). However, relatively little is known about 24-nt phasiRNAs in general besides their functions in anthers. Overall, chromosome 4 remains an enigmatic component of the *Aquilegia* genome, so it is intriguing that the QTL is located on this structure. Certainly, it is also possible that the causal gene underlying Q4 is one of the *Aquilegia*-specific loci that did not have a direct *A. thaliana* homolog, which equally applies to the other QTL as well.

The current study is a key first step in identifying a promising list of candidate genes for regulating natural variation in FMT. The next steps in evaluating these loci will include exploration of fine-mapping, assays of gene function, conducting comparative expression analyses between *A. canadensis* and *A. brevistyla*, and examining sequence variation and patterns of allelic differentiation between populations of these species. Further areas of interest would also include exploring the potential ecological consequences of variation in SWN and FMT between these species and across the genus.

Supplementary data

The following supplementary data are available at *JXB* online.

Fig. S1. SWN and the position of flowers on inflorescences.

Fig. S2. F1-parent-of-origin has a significant impact on the distribution of SWN in the respective F2 progeny.

Fig. S3. Distribution of the SD of SWN among the parental and F2 populations.

Fig. S4. Diagram and summary statistics of the genetic map.

Fig. S5. Confirmation of QTL underlying SWN variation.

Fig. S6. Effect plots of the markers that have the highest LOD score under each QTL.

Fig. S7. Gene phylogeny for *AqROXYa*.

Fig. S8. Gene phylogeny for *AqATH1*.

Table S1. Primers used for constructing *in situ* hybridization probes.

Table S2. Pairwise comparison of FM widths through early developmental stages.

Table S3. No significant evidence supporting the presence of a second QTL on any chromosome.

Table S4. Summary of number of genes under each potential QTL.

Table S5. Expressed genes under Q4.

Table S6. Information on candidate genes.

Acknowledgements

The authors would like to thank Nicole Bedford, Olivia Meyerson, and Rubén Rellán-Álvarez for discussing QTL mapping analysis; Suresh Pokhrel for providing information on miRNA in *Aquilegia*; Pierre Baduel and Rebecca Povilus for discussing data analysis strategies; the graduate students at the Harvard Statistics Department who volunteered their time for professional and free statistics consultation; and Karl Broman for actively answering questions about the R/qtl package on online forums.

Author contributions

YM and EK: conceptualization and design; EB: collection of seeds, crossing and sequencing the parental species, and growing and pollinating the F1 individuals; ME and YM: growing the F2s; YM: conducting all phenotyping; EB, ME, and YM: preparing the libraries for sequencing of the F2 individuals and constructing the genetic map; YM: data analysis and *in situ* hybridization; EK and SH: supervision; YM: writing with input from the co-authors.

Conflict of interest

The authors declare no conflict of interest.

Funding

Funding has been provided by a Simmon's Award to YM from the Harvard Center for Biological Imaging; a National Science Foundation Graduate Research Fellowship under grant no. DGE1745303 to MBE; and both a NIH Ruth L. Kirschstein National Research Service Award (F32GM103154) and a UC Santa Barbara Harvey Karp Discovery award to ESB. Sequencing was carried out by the DNA Technologies and Expression Analysis Cores at the UC Davis Genome Center, supported by NIH Shared Instrumentation Grant 1S10OD010786-01 and the Biological Nanostructures Lab at UC Santa Barbara.

Data availability

All sequence data are deposited in the Sequence Read Archive under BioProject ID PRJNA720109. Scripts and genotype/phenotype data are available upon request. All other data supporting the findings of this study can be found within the paper or within its supplementary data published online.

References

Aköz G, Nordborg M. 2019. The Aquilegia genome reveals a hybrid origin of core eudicots. Genome Biology **20**, 256.

Ballerini ES, Min Y, Edwards MB, Kramer EM, Hodges SA. 2020. POPOVICH, encoding a C2H2 zinc-finger transcription factor, plays a central role in the development of a key innovation, floral nectar spurs, in *Aquilegia*. Proceedings of the National Academy of Sciences, USA **117**, 22552–22560.

Bastida JM, Alcántara JM, Rey PJ, Vargas P, Herrera CM. 2010. Extended phylogeny of Aquilegia: the biogeographical and ecological patterns of two simultaneous but contrasting radiations. Plant Systematics and Evolution **284**, 171–185.

Bollier N, Sicard A, Leblond J, *et al*. 2018. At-MINI ZINC FINGER2 and SI-INHIBITOR OF MERISTEM ACTIVITY, a conserved missing link in the regulation of floral meristem termination in Arabidopsis and tomato. The Plant Cell **30**, 83–100.

Bommert P, Nagasawa NS, Jackson D. 2013. Quantitative variation in maize kernel row number is controlled by the FASCIATED EAR2 locus. Nature Genetics **45**, 334–337.

Brewer PB, Howles PA, Dorian K, Griffith ME, Ishida T, Kaplan-Levy RN, Kilinc A, Smyth DR. 2004. *PETAL LOSS*, a trihelix transcription factor gene, regulates perianth architecture in the *Arabidopsis* flower. Development **131**, 4035–4045

Broman KW, Wu H, Sen S, Churchill GA. 2003. R/qtl: QTL mapping in experimental crosses. Bioinformatics **19**, 889–890.

Cao X, Wang J, Xiong Y, Yang H, Yang M, Ye P, Bencivenga S, Sablowski R, Jiao Y. 2020. A self-activation loop maintains meristematic cell fate for branching. Current Biology **30**, 1893–1904.e4.

Carles CC, Lertpiriyapong K, Reville K, Fletcher JC. 2004. The ULTRAPETALA1 gene functions early in Arabidopsis development to restrict shoot apical meristem activity and acts through WUSCHEL to regulate floral meristem determinacy. Genetics **167**, 1893–1903.

Chu Y, Jang J, Huang Z, van der Knaap E. 2019. Tomato locule number and fruit size controlled by natural alleles of *lc* and *fas*. Plant Direct **3**, e00142.

Ding L, Yan S, Jiang L, Zhao W, Ning K, Zhao J, Liu X, Zhang J, Wang Q, Zhang X. 2015. HANABA TARANU (HAN) bridges meristem and organ primordia boundaries through PINHEAD, JAGGED, BLADE-ON-PETIOLE2 and CYTOKININ OXIDASE 3 during flower development in Arabidopsis). PLoS Genetics **11**, e1005479.

Edwards MB, Choi GPT, Derieg NJ, Min Y, Diana AC, Hodges SA, Mahadevan L, Kramer EM, Ballerini ES. 2021. Genetic architecture of floral traits in bee- and hummingbird-pollinated sister species of *Aquilegia* (columbine). Evolution **75**, 2197–2216.

Endress PK. 1990. Patterns of floral construction in ontogeny and phylogeny. Biological Journal of the Linnean Society **39**, 153–175.

Endress PK. 2011. Evolutionary diversification of the flowers in angiosperms. American Journal of Botany **98**, 370–396.

Fan C, Wu Y, Yang Q, Yang Y, Meng Q, Zhang K, Li J, Wang J, Zhou Y. 2014. A novel single-nucleotide mutation in a CLAVATA3 gene homolog controls a multilocular silique trait in *Brassica rapa* L. Molecular Plant **7**, 1788–1792

Fei Q, Yang L, Liang W, Zhang D, Meyers BC. 2016. Dynamic changes of small RNAs in rice spikelet development reveal specialized reproductive phasiRNA pathways. Journal of Experimental Botany **67**, 6037–6049

Filiault DL, Ballerini ES, Mandáková T, *et al*. 2018. The Aquilegia genome provides insight into adaptive radiation and reveals an extraordinarily polymorphic chromosome with a unique history. eLife **7**, e36426.

Fior S, Li M, Oxelman B, Viola R, Hodges SA, Ometto L, Varotto C. 2013. Spatiotemporal reconstruction of the Aquilegia rapid radiation

through next-generation sequencing of rapidly evolving cpDNA regions. New Phytologist **198**, 579–592.

Galli M, Gallavotti A. 2016. Expanding the regulatory network for meristem size in plants. Trends in Genetics **32**, 372–383.

Gómez-Mena C, Sablowski R. 2008. *ARABIDOPSIS THALIANA HOMEOBOX GENE1* establishes the basal boundaries of shoot organs and controls stem growth. The Plant Cell **20**, 2059–2072.

Greb T. 2003. Molecular analysis of the LATERAL SUPPRESSOR gene in Arabidopsis reveals a conserved control mechanism for axillary meristem formation. Genes & Development **17**, 1175–1187.

Griffith ME, da Silva Conceição A, Smyth DR. 1999. PETAL LOSS gene regulates initiation and orientation of second whorl organs in the Arabidopsis flower. Development **126**, 5635–5644.

Grigorova B, Mara C, Hollender C, Sijacic P, Chen X, Liu Z. 2011. LEUNIG and SEUSS co-repressors regulate *miR172* expression in *Arabidopsis* flowers. Development **138**, 2451–2456.

Hodges SA, Arnold ML. 1994. Columbines: a geographically widespread species flock. Proceedings of the National Academy of Sciences, USA **91**, 5129–5132.

Kakrana A, Mathioni SM, Huang K, *et al*. 2018. Plant 24-nt reproductive phasiRNAs from intramolecular duplex mRNAs in diverse monocots. Genome Research **28**, 1333–1344.

Kim Y-S, Kim S-G, Lee M, *et al*. 2008. HD-ZIP III activity is modulated by competitive inhibitors via a feedback loop in *Arabidopsis* shoot apical meristem development. The Plant Cell **20**, 920–933.

Kramer EM. 2005. Methods for studying the evolution of plant reproductive structures: comparative gene expression techniques. Methods in Enzymology **395**, 617–636.

Kramer EM. 2009. *Aquilegia*: a new model for plant development, ecology, and evolution. Annual Review of Plant Biology **60**, 261–277.

Lampugnani ER, Kilinc A, Smyth DR. 2012. PETAL LOSS is a boundary gene that inhibits growth between developing sepals in *Arabidopsis thaliana*: PTL controls sepal boundaries. The Plant Journal **71**, 724–735.

Lenhard M. 2003. Stem cell homeostasis in the Arabidopsis shoot meristem is regulated by intercellular movement of CLAVATA3 and its sequestration by CLAVATA1. Development **130**, 3163–3173.

Lenhard M, Bohnert A, Jürgens G, Laux T. 2001. Termination of stem cell maintenance in Arabidopsis floral meristems by interactions between WUSCHEL and AGAMOUS. Cell **105**, 805–814.

Li H, Durbin R. 2009. Fast and accurate short read alignment with Burrows–Wheeler transform. Bioinformatics **25**, 1754–1760.

Li H, Handsaker B, Wysoker A, Fennell T, Ruan J, Homer N, Marth G, Abecasis G, Durbin R; **1000 Genome Project Data Processing Subgroup.** 2009. The Sequence Alignment/Map format and SAMtools. Bioinformatics **25**, 2078–2079.

Li S, Lauri A, Ziemann M, Busch A, Bhave M, Zachgo S. 2009. Nuclear activity of ROXY1, a glutaredoxin interacting with TGA factors, is required for petal development in *Arabidopsis thaliana*. The Plant Cell **21**, 429–441.

Li Y, Pi L, Huang H, Xu, L. 2012. ATH1 and KNAT2 proteins act together in regulation of plant inflorescence architecture. Journal of Experimental Botany **63**, 1423–1433

Litt A, Kramer EM. 2010. The ABC model and the diversification of floral organ identity. Seminars in Cell & Developmental Biology **21**, 129–137.

Liu Y, Teng C, Xia R, Meyers BC. 2020. PhasiRNAs in plants: their biogenesis, genic sources, and roles in stress responses, development, and reproduction. The Plant Cell **32**, 3059–3080

Min Y, Conway SJ, Kramer EM. 2022. Quantitative live imaging of floral organ initiation and floral meristem termination in *Aquilegia*. Development **149**, dev200256.

Min Y, Kramer EM. 2017. The *Aquilegia JAGGED* homolog promotes proliferation of adaxial cell types in both leaves and stems. New Phytologist **216**, 536–548.

Min Y, Kramer EM. 2020. Transcriptome profiling and weighted gene coexpression network analysis of early floral development in *Aquilegia coerulea*. Scientific Reports **10**, 19637.

Müller R, Borghi L, Kwiatkowska D, Laufs P, Simon R. 2006. Dynamic and compensatory responses of *Arabidopsis* shoot and floral meristems to *CLV3* signaling. The Plant Cell **18**, 1188–1198.

Munz PA. 1946. *Aquilegia*: the cultivated and wild columbines. Ithaca. NY: Cornell University.

Nardmann J, Werr W. 2006. The shoot stem cell niche in angiosperms: expression patterns of WUS orthologues in rice and maize imply major modifications in the course of mono- and dicot evolution. Molecular Biology and Evolution **23**, 2492–2504.

Ouellette LA, Reid RW, Blanchard SG, Brouwer CR. 2018. LinkageMapView—rendering high-resolution linkage and QTL maps. Bioinformatics **34**, 306–307.

Payne T. 2004. KNUCKLES (KNU) encodes a C2H2 zinc-finger protein that regulates development of basal pattern elements of the Arabidopsis gynoecium. Development **131**, 3737–3749.

Pfluger J, Zambryski P. 2004. The role of *SEUSS* in auxin response and floral organ patterning. Development **131**, 4697–4707.

Pokhrel S, Huang K, Bélanger S, Caplan JL, Kramer EM, Meyers BC. 2021a. Pre-meiotic, 21-nucleotide reproductive phasiRNAs emerged in seed plants and diversified in flowering plants. Nature Communications **12**, 4941.

Pokhrel S, Huang K, Meyers, BC. 2021b. Conserved and non-conserved triggers of 24-nt reproductive phasiRNAs in eudicots. The Plant Journal **107**, 1332–1345.

Ronse De Craene L. 2018. Understanding the role of floral development in the evolution of angiosperm flowers: clarifications from a historical and physico-dynamic perspective. Journal of Plant Research **131**, 367–393.

Ruzin S. 1999. *Plant microtechnique and microscopy*. New York: Oxford University Press.

Sauret-Güeto S, Schiessl K, Bangham A, Sablowski R, Coen E. 2013. JAGGED controls Arabidopsis petal growth and shape by interacting with a divergent polarity field. PLoS Biology **11**, e1001550

Schoof H, Lenhard M, Haecker A, Mayer KFX, Jürgens G, Laux T. 2000. The stem cell population of Arabidopsis shoot meristems is maintained by a regulatory loop between the CLAVATA and WUSCHEL genes. Cell **100**, 635–644.

Schumacher K, Schmitt T, Rossberg M, Schmitz G, Theres K. 1999. The Lateral suppressor (*Ls*) gene of tomato encodes a new member of the VHIID protein family. Proceedings of the National Academy of Sciences,USA **96**, 290–295.

Steeves TA, Sussex IM. 1989. Patterns in plant development. Cambridge: Cambridge University Press.

Sun B, Xu Y, Ng K-H, Ito T. 2009. A timing mechanism for stem cell maintenance and differentiation in the Arabidopsis floral meristem. Genes & Development **23**, 1791–1804.

Thompson AM, Crants J, Schnable PS, Yu J, Timmermans MCP, Springer NM, Scanlon MJ, Muehlbauer GJ. 2014. Genetic control of maize shoot apical meristem architecture. G3 Genes|Genomes|Genetics **4**, 1327–1337.

Thompson AM, Yu J, Timmermans MCP, Schnable P, Crants JE, Scanlon MJ, Muehlbauer GJ. 2015. Diversity of maize shoot apical meristem architecture and its relationship to plant morphology. G3 Genes|Genomes|Genetics **5**, 819–827.

Upadyayula N, da Silva HS, Bohn MO, Rocheford TR. 2006. Genetic and QTL analysis of maize tassel and ear inflorescence architecture. Theoretical and Applied Genetics **112**, 592–606.

Vlăduţu C, McLaughlin J, Phillips RL. 1999. Fine mapping and characterization of linked quantitative trait loci involved in the transition of the maize apical meristem from vegetative to generative structures. Genetics **153**, 993–1007.

Walker-Larsen J, Harder LD. 2000. The evolution of staminodes in angiosperms: patterns of stamen reduction, loss, and functional re-invention. American Journal of Botany **87**, 1367–1384.

Wang Q, Kohlen W, Rossmann S, Vernoux T, Theres K. 2014. Auxin depletion from the leaf axil conditions competence for axillary meristem formation in *Arabidopsis* and tomato. The Plant Cell **26**, 2068–2079.

Weits DA, Kunkowska AB, Kamps NCW, *et al*. 2019. An apical hypoxic niche sets the pace of shoot meristem activity. Nature **569**, 714–717.

Wenkel S, Emery J, Hou B-H, Evans MMS, Barton MK. 2007. A feedback regulatory module formed by LITTLE ZIPPER and HD-ZIPIII genes. The Plant Cell **19**, 3379–3390

Whitewoods CD, Cammarata J, Venza ZN, *et al*. 2020. CLAVATA was a genetic novelty for the morphological innovation of 3D growth in land plants. Current Biology **30**, 2645–2648.

Wynn AN, Seaman AA, Jones AL, Franks RG. 2014. Novel functional roles for PERIANTHIA and SEUSS during floral organ identity specification, floral meristem termination, and gynoecial development. Frontiers in Plant Science **5**, 130.

Xing S, Rosso MG, Zachgo S. 2005. *ROXY1*, a member of the plant glutaredoxin family, is required for petal development in *Arabidopsis thaliana*. Development **132**, 1555–1565.

Xu Q, Li R, Weng L, Sun Y, Li M, Xiao H. 2019. Domain-specific expression of meristematic genes is defined by the LITTLE ZIPPER protein DTM in tomato. Communications Biology **2**, 134.

Yang F, Bui HT, Pautler M, Llaca V, Johnston R, Lee B, Kolbe A, Sakai H, Jackson D. 2015. A maize glutaredoxin gene, *Abphyl2*, regulates shoot meristem size and phyllotaxy. The Plant Cell **27**, 121–131.

Zhai J, Zhang H, Arikit S, Huang K, Nan G-L, Walbot V, Meyers, BC. 2015. Spatiotemporally dynamic, cell-type-dependent premeiotic and meiotic phasiRNAs in maize anthers. Proceedings of the National Academy of Sciences, USA **112**, 3146–3151

Zhao Y, Medrano L, Ohashi K, Fletcher JC, Yu H, Sakai H, Meyerowitz, EM. 2004 HANABA TARANU is a GATA transcription factor that regulates shoot apical meristem and flower development in Arabidopsis. The Plant Cell **16**, 2586–2600